



# Groundwater mixing, nutrient diagenesis, and discharges across a sandy beachface, Cape Henlopen, Delaware (USA)

William J. Ullman<sup>a,\*</sup>, Bonnie Chang<sup>a,b,c,1</sup>, Douglas C. Miller<sup>a</sup>, John A. Madsen<sup>d</sup>

<sup>a</sup>College of Marine Studies, University of Delaware, 700 Pilottown Road, Lewes, DE 19958-1298, USA

<sup>b</sup>Department of Chemistry, University of Virginia, Charlottesville, VA 22903, USA

<sup>c</sup>Department of Environmental Sciences, University of Virginia, Charlottesville, VA 22903, USA

<sup>d</sup>Department of Geology, University of Delaware, Newark, DE 19716, USA

Received 23 May 2002; received in revised form 21 October 2002; accepted 23 October 2002

## Abstract

Groundwater and associated nutrients discharge from the beachface to the Delaware Estuary at Cape Henlopen, Delaware, and appear to contribute significantly to the ecological structure of the adjacent intertidal and subtidal benthic communities. The cross-sectional distributions of salinity and nutrient concentrations at one seepage site indicate that there are two distinct groundwater masses that mix with seawater in the sandy beachface during discharge. The dissolved nutrient concentrations in the beachface at this site are substantially higher than those found in the adjacent estuarine surface water. Nutrient concentrations and distribution in the beachface water reflect: (1) the discharge of nutrient-rich upland water; (2) mixing between nutrient-rich groundwater and estuarine water; and (3) diagenetic recycling of estuarine organic material in the beachface mixing zone. Simple mixing and hydrological models are used to determine the relative magnitude of upland and diagenetic contributions and to estimate absolute nutrient discharges across the beachface. Nutrient fluxes during the summer at this site are sufficient to support carbon fixation rates of 4–17 mol C/m/year along the beachface. These nutrient fluxes are substantially higher than can be supported by the upland discharge alone. This suggests that beachfaces serve as traps and reservoirs of estuarine particulate matter and associated nutrient elements. During the summer, when samples were collected at the Cape Henlopen site, nutrient concentrations in the estuary are low and the remineralization of particles in the beachface may contribute significantly to the productivity of the dense plant and animal communities found adjacent to the beachface.

© 2003 Elsevier Science B.V. All rights reserved.

**Keywords:** groundwater; beachface; nutrients; diagenesis; mixing zones; tidal pumping; coastal aquifer; Delaware Bay

## 1. Introduction

Estuaries receive their primary freshwater input from fluvial discharges, but there is good evidence that direct submarine groundwater discharge may be responsible for up to 10% of the total freshwater input to estuaries and to the ocean (Garrels & Mackenzie, 1971; Zektzer, Ivanov, & Meskheteli, 1973). Until recently, the principal concern associated with the hydrological connection between groundwater and the ocean has

been that associated with saline water intrusion into coastal water supplies (Bear, Cheng, Sorek, Ouazar, & Herrera, 1991; Fetter, 1994). Increasingly, however, there is concern that submarine and marginal marine discharges of nutrient- and contaminant-rich groundwater may have a more significant impact on material fluxes than implied by the relative magnitudes of groundwater and surface water discharges (Burnett et al., 2002; Li, Barry, Stagnitti, & Parlange, 1999; Moore, 1996, 1999; Shaw, 2001; Valiela et al., 1992). Seep zones in many settings appear to be associated with unique and important marginal marine and intertidal biological communities of high productivity (Bussmann, Dando, Niven, & Suess, 1999; Johannes & Hearn, 1985; Page, 1995). Therefore, these discharges may play an important role in local biodiversity, in ecosystem function, and

<sup>1</sup> Present address: School of Oceanography, University of Washington, Seattle, WA 98195, USA.

\* Corresponding author.

E-mail address: [ullman@udel.edu](mailto:ullman@udel.edu) (W.J. Ullman).

potentially in contaminant transfer up the marine and terrestrial (including avian) food chains.

The discharge of groundwater and associated nutrients and contaminants, however, is not a simple advective process. While fluid advection is certainly important, the dispersive mixing of groundwater with seawater, driven in part by tidal pumping and wave swash (Ataie-Ashtiani, Volker, & Lockington, 2001; Baird & Horn, 1996; Lanyon, Eliot, & Clarke, 1982; Li et al., 1999), and the chemical transformations that occur during mixing in the beachface zone may contribute significantly to the impact of groundwater to the seep-associated ecosystem (Uchiyama, Nadaoka, Rölke, Adachi, & Yagi, 2000). Intertidal and subtidal sediments in estuaries are biogeochemically dynamic, and a range of chemical transformations and exchanges between the sedimentary material and interstitial groundwater should be expected as water passes through these reactive sediments and the adjacent beachface.

In this article, we document the dissolved nutrient concentrations in a vertical section across the beachface and adjacent sand flat at a groundwater seepage site in the euhaline region of Delaware Bay (USA) near Cape Henlopen, Delaware. The salinity and dissolved nutrient concentrations in the subsurface at this site confirm that the beachface is an important mixing zone between fresh water and seawater as well as a diagenetically reactive sedimentary system. Mixing between estuarine water and beachface pore and groundwater at such sites is analogous to estuarine mixing between river and seawater, but on much smaller spatial and temporal scales (Moore, 1999). Based on this analogy, mixing models developed for estuarine studies (Officer, 1979; Officer & Lynch, 1981; Smith & Atkinson, 1994) and traditional hydrological arguments are used to infer nutrient fluxes from the beachface to the estuary at the Cape Henlopen seepage site.

## 2. Methods

### 2.1. Site description

Cape Henlopen, Delaware, is a large beach/spit complex located at the intersection of Delaware Bay and the Atlantic Ocean (Fig. 1). The Cape is an active feature characterized by the erosion of its Atlantic margin, its propagation northward toward New Jersey, and the infilling of the intertidal zone behind the propagating spit (Maurmeyer, 1974). There are a number of cycles of beach ridges and dunes associated with the Pleistocene, Holocene, and Modern evolution of the Cape complex (Kraft, 1971). The estuarine water at Cape Henlopen is well mixed, and has salinities typically similar to that of the local coastal ocean (nearby estuarine salinities range from 27 to 30;

Kawabe, Sharp, Wong, & Lebo, 1988). There are seasonal patterns of nutrient concentrations in the estuarine water reflecting nutrient discharges from the Delaware River and estuarine biogeochemistry (Sharp, 1988; Sharp, Culberson, & Church, 1982; Sharp, Pennock, Church, Tramontano, & Cifuentes, 1984).

There are extensive sand flats behind the Cape that are exposed at low tide and are home to an extensive and well-studied benthic community (Bock & Miller, 1995; Karrh & Miller, 1996; Miller, Bock, & Turner, 1992; Miller & Ullman, 2004; Ray, 1989). The brackish-water worm, *Marenzelleria viridis*, is abundant at this site and is associated with high abundances of benthic diatoms and macroalgae, principally *Ulva* sp., and large populations of a number of other intertidal animals. Miller and Ullman (2004) suggest that this community may benefit from lower salinity, seasonal temperature moderation, or nutrient fluxes associated with the local groundwater inputs through the beachface. Thermal infrared imagery collected at this site indicates that there is a remarkable correlation between the distribution of estuarine groundwater seeps (identified by thermal anomalies) and presence of the *M. viridis* community (Miller & Ullman, 2004).

### 2.2. Beach and water-table topography

The beach topography at the sampling site was determined along the 80-m transect by survey based on an arbitrary and distant horizon (Emery, 1961). All vertical data were corrected to true vertical heights relative to the National Geodetic Vertical Datum of 1929 (NGVD29) based on a laser theodolite survey from an National Ocean Survey (NOS) benchmark 400 m east of the site. A minipiezometer was used for water sampling and, where sufficient flow was encountered, was coupled to a potentiometer for the determination of groundwater levels relative to the concurrent tidal heights (Lee, 1977; Winter, Labaugh, & Rosenberry, 1988). Measured groundwater levels were subsequently corrected to true vertical heights relative to NGVD29, using the tide levels and vertical data available for the tidal gauging station located approximately 1 km west of the sampling site (NOS Station 8557380, Lewes, DE). No corrections were made for the difference in density between surface and groundwater as the maximum water-level correction (~4 cm) was small compared with the large differences observed at the site (up to 1 m), and has a negligible impact on the hydraulic gradient calculated from these data.

### 2.3. Water sampling and analysis

Surface and groundwater samples were collected along the sampling cross-section in July 2000 at low

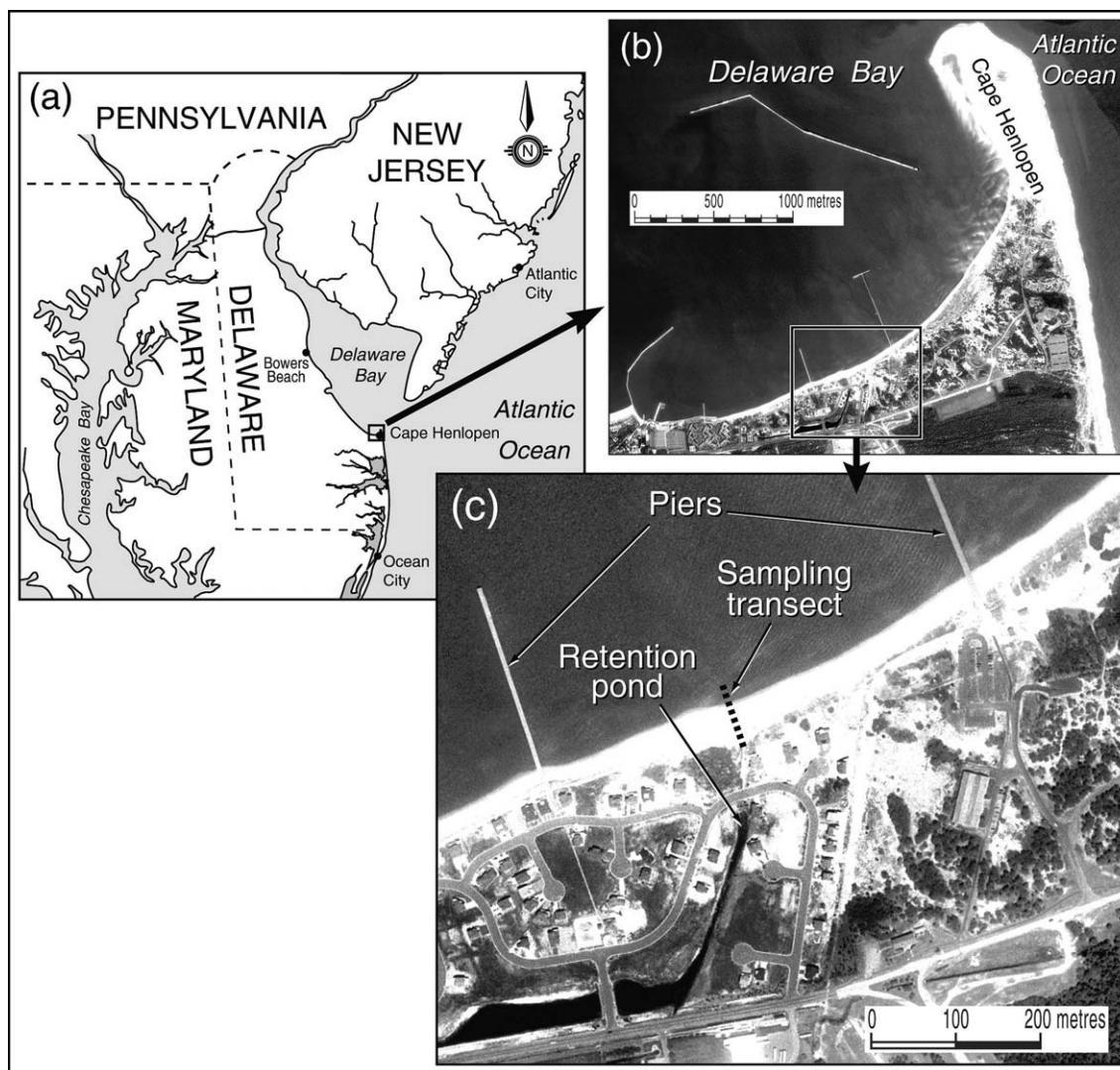


Fig. 1. Location of the Cape Henlopen groundwater seepage site and the sampling transect across which surface and groundwater were collected. Aerial orthophotos taken in 1997, (b) and (c) show the location of the water sampling and GPR transect. The stormwater retention pond discussed in the text is indicated in (c).

water during two successive spring tides. Fourteen groundwater samples were collected on July 2 and 3 when the minimum measured tidal level was 0.12 m below mean low water at the Lewes gauging station. Eight additional surface and groundwater samples were collected on July 16 and 17 when the minimum measured tidal level was 0.3 m above mean low water. The surface-water samples were collected from the estuary 50–100 m offshore of the seepage site and from an up-gradient retention pond (Fig. 1c) using a polyethylene bottle.

Water samples were filtered in the field either through 0.4  $\mu\text{m}$  (pore size) cassette filters, if sample volume was sufficient, or through 0.4  $\mu\text{m}$  in-line filters for smaller samples. Filtered samples were stored on ice in the dark until returned to the laboratory for nutrient analysis. If the analysis could not be performed within 24 h of

collection, the samples were frozen until analysis. The entire analytical work was completed within 6 weeks of collection. Dissolved nutrient concentrations were determined using a Perstorp Analytical Flow Solution Analyzer and standard wet chemical methods. Briefly, nitrate + nitrite ( $\text{NO}_{2+3}^- = \text{NO}_3^- + \text{NO}_2^-$ ) concentrations were determined by the sulfanilamide/*N*(1-naphthyl) ethylene diamine method after cadmium reduction of  $\text{NO}_3^-$  to  $\text{NO}_2^-$ ; ammonium ( $\text{NH}_4^+$ ) was determined by the phenol hypochlorite method; dissolved reactive phosphate ( $\Sigma\text{PO}_4$ ) was determined by the phosphomolybdenum blue method; and silicate ( $\text{Si} = \text{H}_3\text{SiO}_4^-$ ) was determined by the silico-molybdenum blue method (Glibert & Loder, 1977; Grasshoff & Johansen, 1972; Strickland & Parsons, 1972). Dissolved inorganic nitrogen (DIN) was calculated as the sum of  $\text{NO}_{2+3}^-$  and  $\text{NH}_4^+$ . Salinities were determined by conductivity and

are reported with reference to the Practical Salinity Scale of 1978. In one case, where insufficient sample was collected for a complete analysis, only salinity was determined, and this measurement was made by refractometer in the field.

#### 2.4. Beach stratigraphy

Owing to the difficulty in collecting core material from unconsolidated water-saturated sands at this site, ground-penetrating radar (GPR; Beres & Haeni, 1991; Fitzgerald, Baldwin, Ibrahim, & Humphries, 1992; Leatherman, 1987; Meyers, Smith, Jol, & Hay, 1994) was used to determine the subsurface stratigraphy and the thickness of the beachface aquifer for the determination of discharge rates by Darcy's Law (see the subsequent discussion). The data was collected using a Sensors & Software, Inc. (Mississauga, Ontario, Canada) PulseEKKO IV GPR system with 100 MHz antennas and a 400-V transmitter. A GPR cross-section perpendicular to the beach at the groundwater-sampling site was obtained during spring low-tide periods when the beach and sandflat were maximally exposed. Along the survey lines, vertical GPR traces were collected at 1-m intervals with a separation distance of 1.5 m between the transmitter and receiver. Each individual GPR trace consists of 500 amplitude points digitally recorded at a sampling interval of 0.8 ns over a total time interval of 400 ns. At each position along the survey lines, 128 individual amplitude traces were recorded, and the averages of these measurements are reported. These data form the basis of our interpretation of the near-surface stratigraphy at the sampling site.

### 3. Results

#### 3.1. Hydrology and hydrochemistry at the Cape Henlopen site

It is clear from the measured groundwater levels that there are both horizontal and vertical gradients in groundwater levels that would lead to discharges both across and from below the beachface (Fig. 2). Based on the observed water levels, horizontal discharges across the beachface should occur at all tidal heights below mean high water. At the base of the beachface, water levels are consistent with upward seepage during the lower quarter of the mean tidal range. Based on the measured hydraulic heads, the potential for seepage at low tide was detected up to 20 m offshore of the base of the beachface in the swale between intertidal sandbars. The coincidence of discharge and topographic lows in the beach profile is consistent with the thermal infrared imagery at this site, which shows that high-temperature

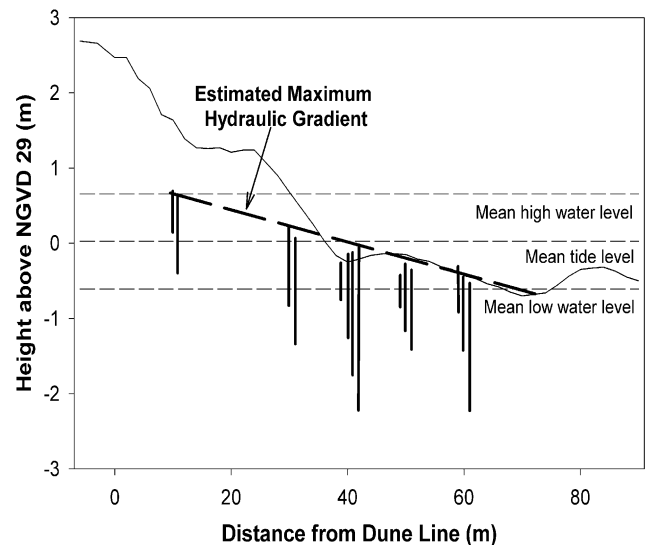


Fig. 2. A two-dimensional section across the beachface at the Cape Henlopen seepage site. Hydraulic heads were determined using a potentiometer. Tidal data are taken from the nearby Lewes gauging station. All vertical data are corrected to NGVD29 using various surveying techniques (see text). The hydraulic gradient shown is the estimated maximum hydraulic gradient used in the Darcy's Law calculation (see text).

anomalies associated with warmer groundwater discharges during the winter occur in the topographic lows adjacent to the beachface (Miller & Ullman, 2004).

Salinity and nutrient concentrations are shown in Fig. 3. Salinity was lowest high on the beachface (within 10 m of the dune line) reflecting the input of fresh groundwater. Higher salinities were found in the upper regions of the sandy beachface and in the surface estuarine water. Low salinities are also found at depth at the base of the beachface and below the first offshore bar (40 to 50 m from the dune line). In the lower intertidal region of the beach (about 20 m offshore of the base of the beachface and 60 m from the dune line), salinity increased with depth reflecting the Ghyben-Hertzberg intrusion of higher density seawater below the lower density freshwater (Fetter, 1994; Freeze & Cherry, 1979).

Based primarily on the distribution of salinity and the relative concentrations of  $\text{NO}_{2+3}^-$  and  $\text{NH}_4^+$  as indicators of redox conditions, the water samples collected at the Cape Henlopen beachface can be grouped as follows (Figs. 4 and 5):

- Surface groundwater (low salinity, high  $\text{NO}_{2+3}^-$  and low in  $\text{NH}_4^+$ ; ▲);
- Deep groundwater (low salinity, low  $\text{NO}_{2+3}^-$ , low  $\text{NH}_4^+$ ; ▼);
- Seawater (high salinity, low  $\text{NO}_{2+3}^-$ , low  $\text{NH}_4^+$ ; ◆);
- Surface-mixed water (intermediate to high salinity, high  $\text{NO}_{2+3}^-$ , low  $\text{NH}_4^+$ ; △);
- Deep-mixed water (low to intermediate salinity, low  $\text{NO}_{2+3}^-$ ; intermediate  $\text{NH}_4^+$ ; ▽); and

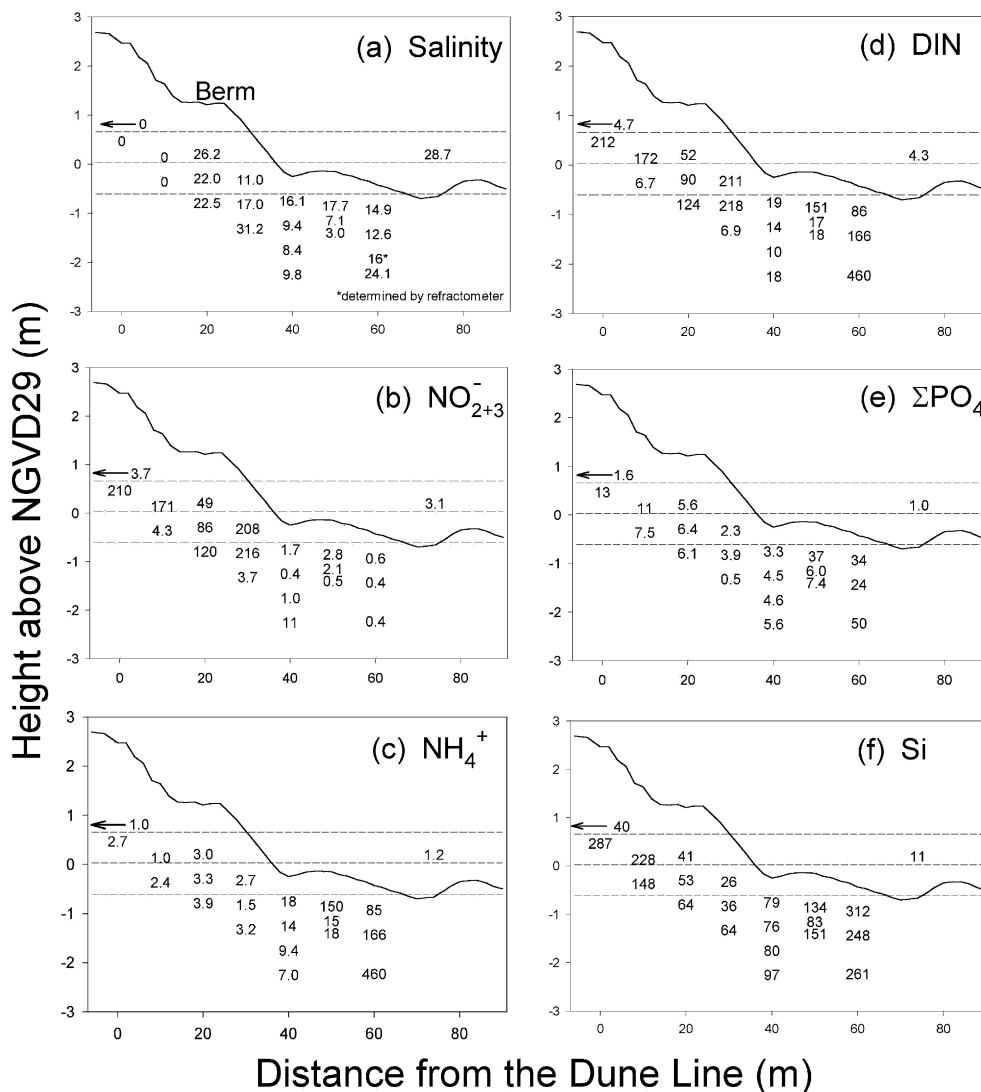


Fig. 3. The cross-sectional distribution of salinity and nutrients in and around the beachface at the Cape Henlopen seepage site. All nutrient concentrations are given in  $\mu\text{M}$ . The horizontal lines show mean high, mean, and mean low tidal levels for Lewes, DE. The arrows show the vertical height and concentration of the up-gradient retention-pond water.

- Sandflat water (intermediate salinity, low  $\text{NO}_{2+3}^-$ , high  $\text{NH}_4^+$ ; ■).

A summary of the chemical characteristics of the various water masses is given in Table 1.

Only a single sample (☆ in Figs. 4 and 5) in the deep subsurface does not clearly fall into one of these classifications. At a salinity of 31.2, this sample is more saline than any other water found at this site. This sample resembles seawater in all respects except Si concentration (see Table 1). The silica concentration, however, is more analogous to the mixed water (both surface and deep) at this site. Due largely to its high salinity, we interpret this water to be a member of the surface-mixed-water class (Fig. 4). However, its origin and history remain unclear. This water may have been produced by the rapid injection of seawater (due to the

formation of salt fingers; Bokuniewicz, 1992) at a time of year when seawater salinity was higher than that during our sampling period. Apparently, this injected water had limited opportunity to mix with the surface groundwater endmember during injection. The conclusions of our study are not dependent on this particular sample or the assignment of this sample to a particular class.

Two of the endmember waters, seawater and the  $\text{NO}_{2+3}^-$ -rich surface groundwater, represent common water that would be found in Delaware’s agriculturally and/or domestically affected coastal zone (Andres, 1991; Kawabe et al., 1988). The  $\text{NO}_{2+3}^-$ -poor deep groundwater does not have a common composition, and the existence of this water may be anomalous to the Cape Henlopen field setting. It is possible that this water is an older groundwater that reflects pre-anthropogenic

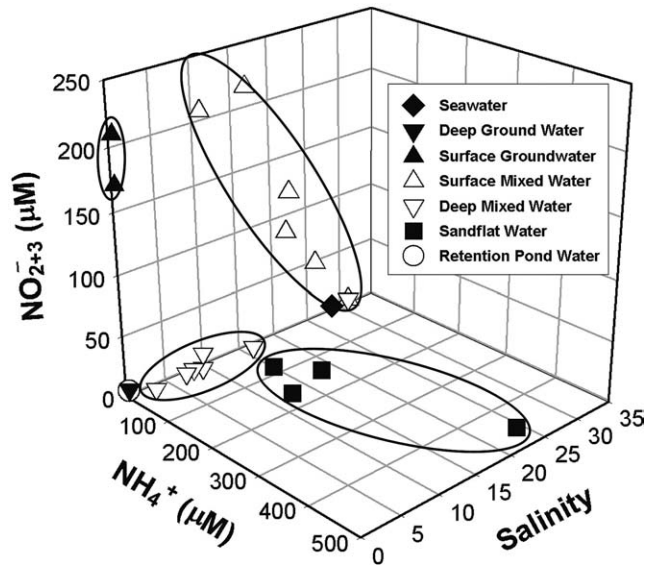


Fig. 4. Water samples showing variations in salinity,  $\text{NO}_{2+3}^-$  and  $\text{NH}_4^+$ , and grouped into water masses as described in Table 1 and consistent with sampled locations and inferred origin.

recharge water, or that has experienced a longer denitrification history than the surface groundwater. Given the high hydraulic conductivity typical of beachface and spit settings and the relatively low Si concentrations found in these waters, this origin is unlikely. Based on the similarities in the observed water chemistry, it is more likely that these waters originate from the stormwater retention pond that presently occupies a streambed that formerly discharged across the dune line at this site. The pond water is hydraulically above the beachface consistent with discharge, is similarly depleted in N species, and has somewhat lower P and Si concentrations than the groundwater (Figs. 3–5; Table 1). The pond composition is due, presumably, to high

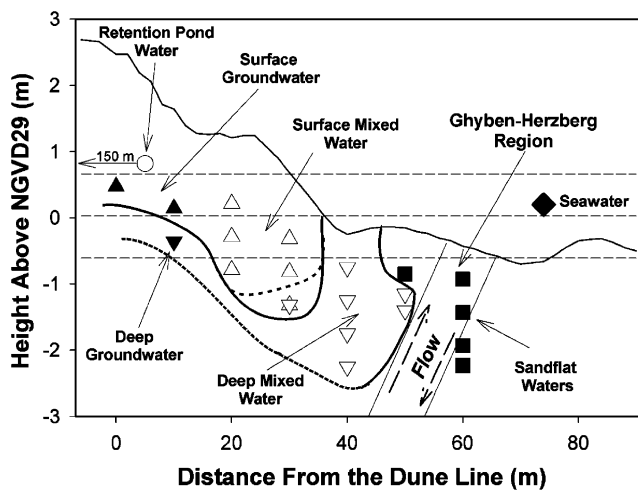


Fig. 5. The spatial distribution of water masses at the Cape Henlopen seepage site. Symbols are as in Fig. 4.

Table 1

The salinity (*S*) and nutrient composition ( $\mu\text{M}$ ) of characteristic water found at or near the Cape Henlopen beachface (see Figs. 4 and 5 and text)

Water mass	<i>S</i>	$\text{NO}_{2+3}^-$	$\text{NH}_4^+$	DIN	$\Sigma\text{PO}_4$	Si
Seawater	28.7	3	1	4	1	11
Deep groundwater	0	4.3	2.4	6.7	7.5	148
Surface groundwater	0	170–210	1–2.7	170–210	11–13	225–290
Surface-mixed water	11–31	50–215	1–3	50–220	2–6	25–65
Deep-mixed water	3–16	0.4–10	7–18	10–19	3–7	75–150
Sandflat water	12–24	0.3–2.8	85–460	85–460	3–50	130–315
Retention-pond water	0	3.7	1	4.7	1.6	39

levels of primary productivity and nutrient uptake in the pond. P and Si, however, are common constituents of sediments and could be picked up by the pond water as it travels through the aquifer to the beachface.

3.2. Beach stratigraphy

The uppermost portion of the GPR cross-section is dominated by two major events (dark reflectors; Fig. 6) that represent electromagnetic (EM) waves that traveled predominantly through the air between the transmitter and receiver. The uppermost, direct airwave marks the ground surface. Beneath the first two airwaves, observed

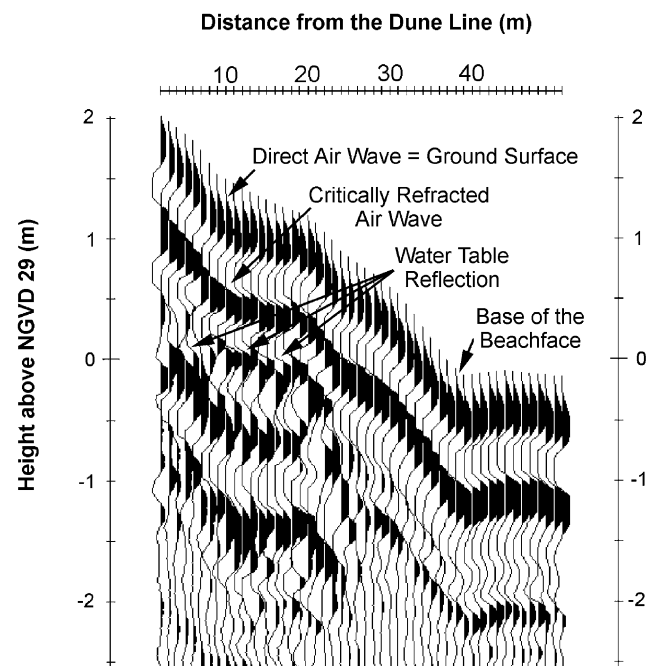


Fig. 6. GPR cross-section along surface and groundwater sampling line showing the inferred stratigraphy and hydrostratigraphy at the Cape Henlopen site. Horizontal scale corresponds to distance from the dune line. Height/depth is relative to NGVD 29. The height/depth scale on the profile was calculated assuming a velocity of 0.08 m/ns for the subsurface GPR waves.

GPR events are associated with changes in the electrical properties (e.g. permittivity, conductivity) of the subsurface materials.

Beginning at the berm (25 m from the dune line) and continuing down the beachface and across the sandflat, there is a noticeable absence of subsurface GPR reflections. The only major reflection in this portion of the cross-section parallels the surface airwaves. This probably is third airwave and is not associated with any subsurface variations in electrical properties. The lack of real subsurface GPR reflections in this portion of the cross-section is most likely due to the effect of saline-saturated sediments, which would obscure the effects of sediment properties on EM wave transmission and/or refraction.

From the dune to the berm lines, however, a series of real subsurface reflection events are observed in the GPR cross-section (Fig. 6). At a depth of approximately +0.1 to +0.2 m (relative to NGVD29) and from 9 to 19 m along the section, a nearly horizontal reflection is observed. Given the nearly horizontal character and its vertical position, this reflection is interpreted to coincide with the water table at the time the survey was made. This depth-to-water-table is consistent with the depth observed at the time of the water sampling (Fig. 2).

Beneath the water table, three additional reflection events are observed in the GPR cross-section (Fig. 6). These events are seen at depths (relative to NGVD29) of approximately 0, -1, and -2 m near the dune line portion of the profile and can be traced oceanward reaching depths of -0.6, -1.5, and -2.6 m, respectively, near the berm line. We interpret these reflectors to be the boundaries that maintain the separation between water masses at this site. The deep penetration of the GPR signal in this region suggests that the pore fluids are predominantly fresh in this region of the beachface, consistent with the observations during sampling (Fig. 3a).

The GPR reflections suggest that there are a series of three distinct sedimentary and hydrostratigraphic layers below the beachface. The uppermost layer, approximately 2 m thick, extends from the surface to a depth of -0.6 m at the berm line (20 m from the dune line) and contains the water table. A second layer of 0.60 m thickness is present at depths between -0.6 and -1.2 m at the berm line. The third layer, approximately 1.4 m thick, extends from depths at the berm line from -1.2 to -2.6 m. The stratigraphy at this site and the sedimentary characteristics of these layers need to be confirmed by direct sediment sampling.

#### 4. Discussion

There are obvious and systematic variations in the nutrient chemistry of the beachface waters at this seepage site. These reflect the input of nitrogen-rich groundwater from the uplands, the complexity of mixing

between two groundwater masses and surface seawater in the beachface discharge zone, and the diagenetic addition of nutrients during the mixing and discharge process. By analogy with estuarine mixing, the relative magnitude of diagenetic additions compared with the direct advective loading of nutrients from the upland groundwater can be assessed using mixing curves (graphs showing the relationship between a reactive constituent compared with a conservative constituent undergoing the same physical mixing regime; Officer, 1979; Officer & Lynch, 1981; Smith & Atkinson, 1994). These results can be coupled with estimates of groundwater discharge at the sampling site to estimate nutrient fluxes to the estuary through the beachface.

##### 4.1. Mixing curves

Fig. 7 shows mixing curves for nutrients analyzed in this study. The  $\text{NO}_{2+3}^-$  mixing curve (Fig. 7a) indicates that there are three distinct endmembers, consistent with the observed grouping of samples, in this beachface-mixing regime. Surface seawater represents one endmember. This endmember mixes with the  $\text{NO}_{2+3}^-$ -poor deep groundwater to yield the deep-mixed water (see Figs. 3 and 5). The seawater endmember also mixes with the  $\text{NO}_{2+3}^-$ -rich surface groundwater to yield the surface-mixed water. These two mixing trends appear to be distinct and independent, consistent with the distinct regions of the beachface where the relevant samples were collected (Fig. 5).

The surface-mixed water shows  $\text{NO}_{2+3}^-$  concentrations higher (as indicated by  $\Delta$  above the solid mixing line shown in Fig. 7a) than can be accounted for by mixing of the observed endmembers and is consistent with  $\text{NO}_{2+3}^-$  production during mixing. The deep-mixed water shows little or no evidence of consumption or production of  $\text{NO}_{2+3}^-$  during mixing; however, intermediate levels of  $\text{NH}_4^+$  are found in these waters. While the intermediate levels of  $\text{NH}_4^+$  might result from the mixing of sandflat water and deep groundwater, this mixing mechanism is not evident from the distribution of either  $\Sigma\text{PO}_4$  or Si. This suggests that the intermediate levels of  $\text{NH}_4^+$  result from ammonification along the deep groundwater-seawater mixing pathway and not mixing alone ( $\nabla$  above the mixing line shown in Fig. 7b). Apparently, nitrogen release to beachface water occurs both under oxic ( $\text{NO}_{2+3}^-$ -dominated) and anoxic ( $\text{NH}_4^+$ -dominated) conditions at this site.

Presumably, the production of  $\text{NO}_{2+3}^-$  in the surface-mixed water is associated with oxic respiration during mixing across the beachface. Significant  $\text{NO}_{2+3}^-$  enrichment by respiration requires both a source of reduced nitrogen (either as  $\text{NH}_4^+$  or as dissolved or particulate organic N) and dissolved oxygen as reactants. The frequent tidal and wave inundation coupled with filtration of wave-suspended and other estuarine particles

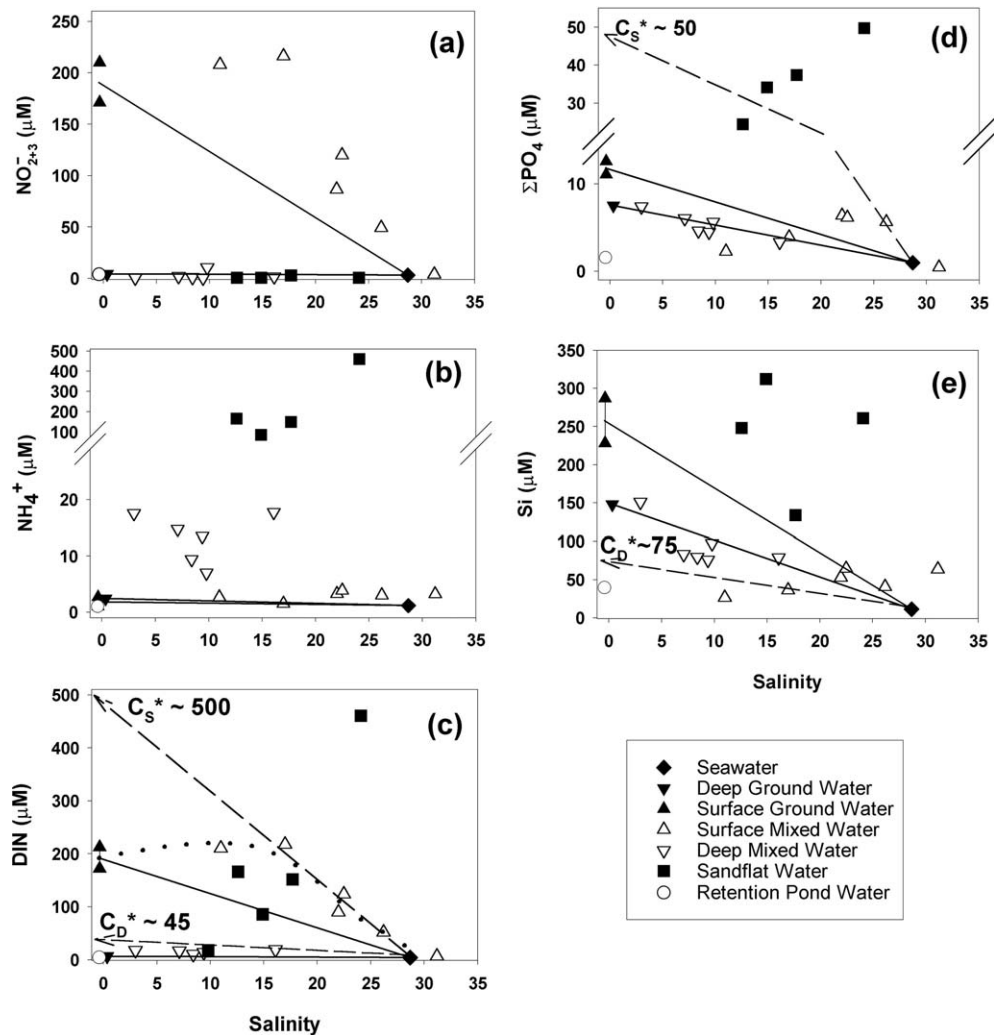


Fig. 7. Mixing curves showing the effect of mixing and reaction during mixing. The composition of the hypothetical surface groundwater endmember (see text) is shown in (a). Linear mixing curve connecting the endmembers for the two observed mixing trends (—) and a curve showing evidence of net nitrogen production during mixing (· · ·) is given in (c). The values of  $C^*$  used to determine the flux of nutrient elements out of the beachface to estuarine water are determined by extrapolating from the tangent to the mixing curve at high salinity to  $S = 0$  (---).

(seston and plankton) would provide a persistent source of locally produced and reactive organic matter and simultaneously maintain the oxic conditions needed for this respiration pathway. Dissimilatory  $\text{NO}_3^-$ -reduction can largely be discounted as a source of  $\text{NH}_4^+$  in the deep-mixed zones, as the total DIN concentration ( $\text{DIN} = \text{NO}_{2+3}^- + \text{NH}_4^+$ ) does not remain constant (Fig. 7c). In addition, the available  $\text{NO}_{2+3}^-$  in these regions of the beachface cross-section is insufficient to sustain such high concentrations of  $\text{NH}_4^+$  by this mechanism alone (Fig. 7a).

Slight enrichment of  $\Sigma\text{PO}_4$  is also observed in some regions of the upper beachface where oxic respiration is observed by the enrichment of  $\text{NO}_{2+3}^-$ .  $\Sigma\text{PO}_4$  release to solution should also accompany oxic respiration. Apparently,  $\Sigma\text{PO}_4$  release rates in the oxic zone are sufficiently high to overcome the absorptive scavenging of  $\Sigma\text{PO}_4$  onto particles coated with iron oxide or

hydroxide phases (Krom & Berner, 1980), particles that we observed commonly at this site (Miller & Ullman, 2004). Interestingly, Si also appears to be released to solution in some of the same regions of sandflat where  $\text{NH}_4^+$  and  $\Sigma\text{PO}_4$  concentrations are elevated (Fig. 7e). The apparently high rates of Si release to solution during sandflat diagenesis may be related to the high abundance of benthic diatoms in the nearby subtidal and intertidal zones. N, P, and Si are fixed by benthic diatoms on the sandflat and may subsequently be remineralized together in the sediments on death and burial in the beachface. Although the mechanisms of Si remineralization are not identical to those responsible for N and P remineralization, the processes are often spatially and temporally correlated. Heterotrophs responsible for N and P remineralization may also produce metabolic compounds that incidentally enhance Si remineralization (Ullman & Welch, 2002). There is

also evidence of Si scavenging (consumption) in some parts of the surface and deep-mixed zones. Scavenging and release of Si in these beachface sediments may be related to the dissolution and precipitation of iron oxyhydroxides onto which Si may adsorb (Hansen, Wetsche, Raulund-Rasmussen, & Borggaard, 1994; Vempati & Loeppert, 1989).

#### 4.2. Diagenetic enhancement of nutrient discharges

Mixing curves may also be used to estimate the relative flux of nutrients to the beachface from the upland and out of the beachface to the estuary (Officer, 1979; Officer & Lynch, 1981; Smith & Atkinson, 1994). In this analysis, as in typical estuarine applications, salinity is used as the conservative property and the composition of mixing endmembers is assumed to be constant or vary only slowly compared with the rate of mixing. The average net rate of groundwater discharge and the rates of nutrient transformations are also assumed constant. The mixing regime, however, can vary with time as long as mixing affects the conservative and reactive tracers identically. High-frequency fluctuations in the discharge due to wave and tidal period processes are components of the mixing regime and do not affect the average net discharge.

In the Officer mixing model (Officer, 1979; Officer & Lynch, 1981), the advective input of a dissolved reactive constituent from land to the mixing zone,  $F_i$ , is given by:

$$F_i = QC_i \quad (1)$$

where  $Q$  is the net discharge and  $C_i$  is the concentration of the constituent entering the mixing zone from the uplands. The output of the reactive constituent from the mixed zone to the receiving body,  $F^*$ , is given by:

$$F^* = Q \left[ C_o - S_o \left( \frac{\partial C}{\partial S} \right)_o \right] = QC^* \quad (2)$$

where  $C_o$  is the concentration of the constituent,  $S_o$  is the salinity, and  $(\partial C/\partial S)_o$  is the slope of the mixing curve, all at the point where the constituent is discharged into the receiving body.  $C^*$  ( $= C_o - S_o(\partial C/\partial S)_o$ ) is an effective advective discharge concentration that can be graphically estimated by extrapolating the tangent of the mixing curve at high salinities to  $S = 0$  (dashed lines in Fig. 7; Officer, 1979). Under these circumstances, the relative enhancement of discharge due to addition or removal from the mixed water during mixing is given by:

$$R = \frac{F^*}{F_i} = \frac{C^*}{C_i} \quad (3)$$

Note that the discharge rate,  $Q$ , is not needed to calculate the relative contributions of the initial input water and that due to subsequent reaction to the total constituent discharge, although it is ultimately needed to

calculate absolute fluxes of the constituent. The incremental fraction of the reactive constituent added to solution in the mixing zone,  $f$ , is given by:

$$f = \left[ \frac{F^* - F_i}{F_i} \right] = \frac{C^* - C_i}{C_i} = (R - 1) \quad (4)$$

This fraction represents the addition or removal of a reactive constituent by processes other than mixing; In this setting,  $F^* - F_i$  reflects the diagenetic contribution of the beachface to material discharge.

The data collected and the mixing curves for DIN,  $\Sigma\text{PO}_4$ , and Si were analyzed to determine  $R$  and  $f$  for the mixing line between seawater and surface groundwater (labeled with subscript S) and the mixing line between seawater and the deep groundwater (labeled with subscript D; Table 2). The sandflat water in the intertidal zone are ignored in this analysis as they reflect nutrient contributions due to subtidal sedimentary processes rather than beachface processes. However, the impact of the beachface hydraulic gradient (Fig. 2) on the fluxes from this zone may enhance diagenetic recycling rates over those that might be expected in the absence of an imposed hydraulic flux.

Although there is considerable uncertainty in the determination of  $(\partial C/\partial S)_o$  and therefore in the estimation of  $C^*$ ,  $R$ , and  $f$ , this analysis clearly indicates that there are substantial diagenetic additions of nutrients to the beachface water that discharge into the estuary at the Cape Henlopen seepage site. The high rates of discharge are consistent with the high abundances of primary producers and consumers at this site, both of which benefit from and are potentially responsible for these diagenetic loadings (see the subsequent discussion). However,  $F_i$ , the nutrient flux into the beach from the upland and  $F^*$ , the flux out of the beach to the estuary, cannot be estimated without an estimate of average net groundwater discharge,  $Q$ .

Table 2

The relative importance of upland discharges and diagenetic releases to the nutrient discharges from the beachface at the Cape Henlopen seepage site<sup>a</sup>

Material	$C_i$ ( $\mu\text{M}$ )	$C^*$ ( $\mu\text{M}$ )	$R = C^*/C_i$	$f = R - 1$
DIN ( $F_S$ )	192	500	2.6	1.6
DIN ( $F_D$ )	6.7	45	6.7	5.7
Phosphate ( $F_S$ )	11.5	50	4.3	3.3
Phosphate ( $F_D$ )	7.5	7.5	1	0
Silicate ( $F_S$ )	260	260	1	0
Silicate ( $F_D$ )	150	75	0.5	-0.5 <sup>b</sup>

<sup>a</sup> The diagenetic water found offshore of the beachface is not considered in this analysis.  $R$  is the relative magnitude of the total discharge to the estuary compared with the upland contribution and  $f$  is the relative magnitude of the upland and diagenetic contributions (Eqs. (3) and (4)).  $C^*$  (Eq. (2)) was graphically estimated from the individual mixing curves (see Fig. 6).

<sup>b</sup> Negative values of  $f$  indicate a flux into the sediment. At this site, the negative flux may reflect Si uptake by benthic diatoms.

### 4.3. Absolute discharge of water and nutrients

The horizontal discharge of water from the beachface can be estimated from Darcy's Law:

$$Q = KD \left( \frac{dh}{dl} \right) \quad (5)$$

where  $Q$  is the discharge per unit length of beachface,  $dh/dl$  is the hydraulic gradient, which can be determined from the measured hydraulic heads at this site,  $D$  is the thickness of the water-containing permeable unit(s), and  $K$  is the horizontal hydraulic conductivity. All of the parameters necessary to calculate discharge may be measured or estimated for the conditions at the Cape Henlopen seepage site.

Well-sorted sands have hydraulic conductivities between 1 and  $10^3$  m/day and silty sands may have hydraulic conductivities as low as  $10^{-2}$  m/day (Freeze & Cherry, 1979). A more constrained estimate of conductivity can be estimated from the grain size distribution (Fetter, 1994). On the upper intertidal sections of the Cape Henlopen beachface, sands are locally well sorted but have a variable median grain size ranging from 350 to 750  $\mu\text{m}$  (Demarest, 1978). At the base of the beachface, the sediment is less well sorted and the predominant sand size is 250  $\mu\text{m}$  (ranging from 200 to 300  $\mu\text{m}$ ; Ray, 1989). Based on these data, the Shepherd (1989) method yields a hydraulic conductivity in the range of 75–300 m/day for the upper part of the beachface where the predominant mixing between the surface groundwater and seawater takes place. The estimated hydraulic conductivity of lower beachface, where the lower mixed water exchange with seawater, ranges from 30 to 60 m/day. The Shepherd (1989) method yields estimates of  $K$  that are consistent with the hydraulic conductivities typical of fine- to medium-sand bodies and typical of the precision of direct measurements of  $K$  for such bodies (Landon, Rus, & Harvey, 2001).

The thickness of the permeable units,  $D$ , is constrained by the sampling and by the GPR results. High on the beachface, at the site 10 m from the dune line, the surface groundwater was sampled at 1.5 m and the deep groundwater at 2 m below land surface. The thickness of the surface discharge zone ( $D_S$ ) is constrained to be, at minimum, the depth from the water table ( $\sim 1$  m below land surface) to the sampling depth at which the surface groundwater was collected ( $D_S$  (min) = 0.5 m) and, at maximum, the depth from the water table to the depth at which the deep groundwater was found ( $D_S$  (max) = 1 m). The minimum thickness of the lower zone ( $D_D$ ) is the difference between the two sampling depths at this site ( $D_D$  (min) = 0.5 m). Because no sampling was done below the 2 m depth, no maximum limit for  $D_D$  can be estimated based on the water sampling.

Based on the GPR results, the difference between the depth to the water table (first significant reflector; see Fig. 6) and the base of the upper layer (second significant reflector),  $D_S$  is approximately 0.6 m. The deep-water mixing zone is represented by the interval between the second and third GPR reflectors and has a maximum depth of 0.6 m. The deepest layer identified by GPR was not sampled for water chemistry or hydraulic properties. Because of the uncertainty associated with the GPR analysis,  $D_S$  is estimated primarily from the observations at the time of water sampling ( $D_S = 0.75$  m, the mean of the inferred minimum and maximum).  $D_D$  is taken to be 0.5 m, based on the minimum depth from the water sampling and the maximum depth estimated from the GPR results. Due to the large uncertainties in the hydraulic conductivities of these sediments, the uncertainties in  $D_S$  and  $D_D$  do not greatly affect the magnitude of the discharge calculated from Darcy's Law (Eq. (5)).

Although there are complexities in the distribution of water levels in a tidal beachface (Ataie-Ashtiani et al., 2001), the hydraulic gradient at this site can be estimated with sufficient precision for the determination of average discharges based on the measured hydraulic heads. The minimum gradient will occur when the tide is at its highest water level. We use the mean high water level as an estimate of this value; and based on the measured heads, the gradient at this tide level would be negligible. The maximum gradient would occur at the lowest tide level. Mean low water is taken as an estimate of this level. The maximum gradient was found to be  $0.024 \pm 0.005$ . Half of this maximum value,  $0.012 \pm 0.002$ , is taken to be the mean tidally averaged gradient at this site for the purpose of calculating water discharge and associated nutrient fluxes. These estimates of the hydraulic gradient across the beachface are primitive, but are of sufficient precision for the calculation of average discharges, given the uncertainties in the estimates of hydraulic conductivities at this site.

Using the previously estimated parameters for the Darcy equation (Eq. (5)), the calculated ranges of discharge across the beachface and the nutrient fluxes associated with this discharge are given in Table 3. The estimated total water discharge rate from the beachface ranges between 0.7 and  $3.6 \text{ m}^3/\text{m}/\text{day}$  with this uncertainty resulting largely from the uncertainty in the determination of hydraulic conductivity. While this estimate of discharge is higher than many previous reports, it is consistent with observations made at a similar sandy site by Bokuniewicz and Zeitlin (1980) where discharge occurs across a broader expanse of the intertidal and subtidal that at the Cape Henlopen Site.

A second, geometric estimate of discharge can be determined based on the difference between the water content of the sandy beachface sediments at high and low tides to confirm that the estimated Darcy flux is

Table 3  
Groundwater discharge and associated nutrient fluxes across the beachface at the Cape Henlopen site<sup>a</sup>

Material	$C_i$ ( $\mu\text{M}$ )	$C^*$ ( $\mu\text{M}$ )	$Q$ ( $\text{m}^3/\text{m}/\text{day}$ )	$F_i^b$ (mol/m/day)	$F^*$ (mol/m/day)
Water ( $Q_S$ )			0.6–3.2		
Water ( $Q_D$ )			0.1–0.4		
Total water ( $Q_S + Q_D$ )			0.7–3.6		
Nitrogen ( $F_S$ )	192	500		0.1–0.6	0.3–1.6
Nitrogen ( $F_D$ )	6.7	45		0.001–0.003	0.006–0.01
Total nitrogen ( $F_S + F_D$ )				0.1–0.6	0.3–1.6
Phosphorus ( $F_S$ )	11.5	50		0.006–0.04	0.03–0.16
Phosphorus ( $F_D$ )	7.5	7.5		0.001–0.003	0.001–0.003
Total phosphorus ( $F_S + F_D$ )				0.007–0.04	0.03–0.16
Silica ( $F_S$ )	260	260		0.14–0.8	0.14–0.8
Silica ( $F_D$ )	150	75		0.02–0.06	0.01–0.03
Total silica ( $F_S + F_D$ )				0.16–0.9	0.15–0.8

<sup>a</sup>  $C^*$  (Eq. (2), Fig. 6) was graphically estimated (see text). Hydraulic conductivities, the thicknesses of the upper and lower layers, and the hydraulic gradient are given in the text. In each calculation, the range given is that calculated from the minimum and maximum values of the parameters in Eq. (5). All discharges and fluxes are given with respect to 1 m along the beachface at the discharge zone.

<sup>b</sup> Estimates of  $F_i$  reflect upper bounds.

reasonable. At mean high tide, the sandy beachface sediments from the 10 to 40 m mark (Fig. 2) are saturated and would contain approximately 7.9–10.1 m<sup>3</sup>/m of water between the high- and low-water marks (based on an estimated porosity range of 0.35–0.45 for this site). At mean low tide, assuming a linear decrease in the water table between 10 and 40 m and a complete drainage of water from this zone of the beachface, the volume of water remaining between the high- and low-water marks would be from 5.1 to 6.5 m<sup>3</sup>/m. The difference between these upper and lower limits, 2.8–3.6 m<sup>3</sup>/m, is a geometric estimate of the maximum discharge of water due to complete drainage of the saturated sediments resulting from the drop in tidal level. Of course, complete drainage of the beachface is not likely to occur due to adsorption of water and capillary processes. The minimum field capacity (water retained on extensive drainage) of fairly clean sand is approximately 15% of the total saturated porosity (Marshall, Holmes, & Rose, 1996), which reduces the estimated maximum discharge volume to 2.4–3.1 m<sup>3</sup>/m per tidal cycle. There are approximately two tidal cycles per day yielding a daily geometric discharge estimate of 4.8–6.1 m<sup>3</sup>/m/day. This estimate is somewhat larger than the hydraulic estimate of discharge and this discrepancy probably reflects the incomplete drainage of the beachface during a tidal cycle (Ataie-Ashtiani et al., 2001). The geometric estimate, however, serves to confirm that the hydraulic estimates of discharge and the nutrient fluxes determined from these estimates are not unreasonable.

The hydraulic and geometric estimates of discharge to the estuary include both the contributions from new fresh groundwater inputs and from recycled seawater. This discharge is subsequently used to calculate both the nutrient fluxes from the freshwater input to the beachface and the total discharge from the beachface to the estuary. The freshwater discharge, however, is likely to be smaller than the total discharge as the slope of the

water table in the upper region of the beachface is likely to be overestimated from the extrapolation of the hydraulic gradient from the lower portions of the beachface. As a result, the estimates of  $F_i$  determined from the total discharge reflect upper bounds.

#### 4.4. Ecological implications

The reported fluxes of N and P to Delaware Bay from the Cape Henlopen site (Table 3) are fairly high and are capable of supporting the high levels of benthic biomass found adjacent to the site. Using the average C/N (=6.25) and C/P (=106) ratios for marine plankton (Redfield, Ketchum, & Richards, 1963; Valiela, 1995), the discharges of N and P could locally support a maximum carbon fixation rate of up to between 4 and 17 mol C/day/m of shoreline. If we presume that the effect of this discharge impacts primarily the *M. viridis* zone within 20 m of the base of the beachface (Miller & Ullman, 2004) and that this flux could be maintained over the whole year, the discharge of nutrients from the beachface could support an equivalent of 70–310 mol C/m<sup>2</sup>/year (0.8–3.7 kg C/m<sup>2</sup>/year). While these areal productivity estimates are higher than typical marine values, they are not unreasonable for the rates of carbon fixation in benthic microalgal communities (Valiela, 1995). However, the fluxes reported in this study were measured near the highest annual temperatures that occur at this site and therefore should represent maximum and not mean annual nutrient fluxes. Thus, the calculated rates of potential carbon fixation represent maximum-daily and not mean annual rates. The average would be expected to be much lower than these maximum estimates, given the exponential dependence of microbially mediated nutrient regeneration on temperature (Aller & Yingst, 1980; Klump & Martens, 1983). It should also be recognized that such groundwater discharge sites are not uniformly distributed along

Delaware Bay (Miller & Ullman, 2004) and that the localization of the impact of these fluxes to a uniform intertidal zone within 20 m of the shoreline is perhaps an unreasonable idealization. These fluxes, however, should, and apparently do, have an impact on the productivity near the discharge site as observed by the high levels of benthic biomass in the forms of primary producers (diatom mats and macroalgae) and consumers (*M. viridis* and other organisms, see the earlier discussion).

#### 4.5. Spatial and temporal patterns of diagenesis and discharge

At the Cape Henlopen sampling site, two distinct groundwater masses meet, mix, and discharge. However, this may not be a common occurrence on the typical estuarine coastline. Hydrogeology analogous to the upper groundwater situation at the Cape Henlopen site is likely to be found at any site where seepage occurs. However, the deep discharge system observed at this site, and from which a substantial nutrient flux is observed (Table 3), is unlikely to occur at many other beachface sites, although offshore discharges may be associated with deeper groundwater systems. At the Cape Henlopen beachface, however, the bulk of the observed nutrient discharge (>80% for Si and >90% for N and P; Table 3) is associated with the surface and not the deep groundwater mass. Therefore, we presume that groundwater and associated nutrient fluxes similar to those found at the Cape Henlopen site may be found at other seepage sites in Delaware and elsewhere where they may have similar and similarly significant ecological effects.

Based on the thermal infrared survey of the southwestern margin of Delaware Bay (Miller & Ullman, 2004), sites where groundwater discharges in large quantities across the beachface were only abundant at Cape Henlopen, where the spit/barrier beach is wide enough to support a substantial freshwater table. We have not surveyed other areas where such seepage might be found along the Delaware Bay; but based on the analysis of coastal geomorphology (principally the presence or absence of salt marshes and wide barrier beaches), it is unlikely that extensive discharge of water from the surficial aquifer to the bay through the beachface will be found at many additional locations. At present, we conclude that extensive direct groundwater seepage from the water-table aquifer to the estuary through the beachface is probably limited to the Cape Henlopen region of Delaware Bay. Nonetheless, some seepage should be expected along any beachface. Seepage to marshes may also be important in many areas of the Delaware Estuary (Page, 1995; Tobias, Macko, Anderson, Canuel, & Harvey, 2001), and offshore discharges may also be present.

However, since nutrient fluxes from the beachface to the adjacent estuary reflect both the upland discharges and diagenetic remineralization of sedimentary particles, the diagenetic nutrient fluxes may be maintained even in the absence of extensive upland discharge. At the Cape Henlopen site, the bulk of the N and P discharge is due to the diagenetic contribution ( $f = 60\text{--}85\%$  for N;  $f = 75\%$  for P; see Eq. (4) and Tables 2 and 3) and this component of the beachface discharge of nutrients may be independent of the rate of groundwater discharge from the upland.

It is intriguing to speculate on the source of the reactive organic matter in the beachface that is needed to support the nutrient fluxes observed at this site. Presumably, the bulk of the organic matter is produced nearby and is washed up onto the beach due to swash and wave-induced resuspension, coupled with the tidal cycle. Under these conditions, the percolating water is filtered by the beach sands, leaving behind the locally produced and reactive organic matter for subsequent diagenetic recycling. The swash-filtering process provides not only organic carbon (and silica in the form of diatom tests), but also a constant source of oxygen needed to sustain the high rates of nitrification in the upper beachface. Although total organic carbon levels in beach sands are normally low, the evidence of high levels of nutrient remineralization suggests that the organic matter that is present is highly reactive, suggesting a local origin. In a recent study, D'Andrea, Aller, and Lopez (2002) demonstrated high dissolved carbon and nitrogen remineralization rates from similar intertidal sediments in South Carolina. They reported nitrogen fluxes of up to  $6.5 \text{ mmol/m}^2/\text{day}$  from these sediments during the summer based on a closed system incubation and suggest that this value represents a minimum due to the elimination of advective inputs and exchange. If the diagenetic inputs of nitrogen to the Delaware Estuary at Cape Henlopen ( $F^* - F_i$ ; see Table 3) are normalized to the 30 m width of the beachface, the resulting areal fluxes ( $6.5$  to  $30 \text{ mmol/m}^2/\text{day}$ ) are comparable with those found in South Carolina. Boudreau et al. (2001) have similarly suggested that high levels of respiration and organic degradation should be expected in shelf sands in productive regions owing to filtration and aeration. This is in spite of the low levels of organic carbon found in such sedimentary settings.

The beachface may also serve as a nutrient reservoir for the adjacent estuary when trapping exceeds remineralization. Water and associated organic particles flow from the estuarine water into the beachface during all times of the year. Diagenetic remineralization is temperature dependent and, therefore, is highest in the summer months. Thus, particulate nutrient inputs have the potential of being stored in the beachface during the winter to support primary productivity during the following summer.

## 5. Summary

At Cape Henlopen, Delaware, a site with high levels of groundwater discharge across the beachface owing to contributions from the upland to tidal drainage, and to wave swash was identified. These discharging waters have, in addition, high levels of N and P due, in part, to contributions associated with the remineralization of reactive organic matter. These lead to N and P fluxes to the estuary substantially higher than can be sustained by upland discharges alone. There is strong evidence of ammonification in the deeper zones of the beachface. Higher on the beachface, nitrification is the dominant process. Nitrification is sustained by the aeration from tidal pumping and wave swash. Although such discharge sites are not common along the Delaware Bay beachface, they represent a potential, locally important source of nutrients at all times of the year.

## Acknowledgements

B.C. was supported during the summer of 2000 by an NSF-REU fellowship administered by J. H. Sharp. Funding from the Delaware Sea Grant College Program to W.J.U., D.C.M., and J.A.M. supported the bulk of the field and analytical work. The USEPA CISNet Program (STAR Grant R826945, W.J.U., Project Director), supported some of the equipment costs for this project. The authors thank the Cape Shores Homeowners Association and the Delaware Department of Natural Resources and Environmental Control (Division of Soil and Water) for permission to work at this site and for their tolerance. This work was completed while W.J.U. was a visiting scientist at CSIRO Land and Water and at the School of Chemistry, Physics, and Earth Sciences at Flinders University, Adelaide, South Australia. Critical reviews of this manuscript by S. Lamontagne, I. Bussmann, and two anonymous reviewers are gratefully acknowledged.

## References

- Aller, R. C., & Yingst, J. Y. (1980). Relationship between microbial distributions and the anaerobic decomposition of organic matter in surface sediments of Long Island Sound, U.S.A. *Marine Biology* 50, 29–42.
- Andres, A. S. (1991). *Ground-water level and chemistry data for the coastal Sussex County, Delaware Ground-water Quality Survey* (31 pp.). Open File Report 33 Delaware Geological Survey, Newark.
- Ataie-Ashtiani, B., Volker, R. E., & Lockington, D. A. (2001). Tidal effects on groundwater dynamics in unconfined aquifers. *Hydrological Processes* 15, 655–669.
- Baird, A. J., & Horn, D. P. (1996). Monitoring and modeling groundwater behaviour in sandy beaches. *Journal of Coastal Research* 12, 630–640.
- Bear, J., Cheng, A. H.-D., Sorek, S., Ouazar, D., & Herrera, I. (Eds.), (1991). *Seawater intrusion in coastal aquifers: Concepts, methods, and practices*. Dordrecht: Kluwer.
- Beres, M., & Haeni, F. P. (1991). Application of ground-penetrating radar methods in hydrogeologic studies. *Ground Water* 29, 19–22.
- Bock, M. J., & Miller, D. C. (1995). Storm effects on particulate food resources on an intertidal sandflat. *Journal of Experimental Marine Biology and Ecology* 187, 81–101.
- Bokuniewicz, H. J. (1992). Analytical descriptions of subaqueous groundwater seepage. *Estuaries* 15, 458–464.
- Bokuniewicz, H. J., & Zeitlin, M. J. (1980). *Characteristics of the ground-water seepage into Great South Bay* (37 pp.). Marine Science Research Center, State University of New York at Stony Brook, Stony Brook, Special Report No. 35.
- Boudreau, B. P., Huettel, M., Forster, S., Jahnke, R. A., MacLachlan, A., Middelberg, J. J., Nielson, P., Sansone, F., Taghon, G., Van Raaphorst, W., Webster, I., Weslawski, J. M., Wiberg, P., & Sundby, B. (2001). Permeable marine sediments: overturning an old paradigm. *EOS, Transactions, American Geophysical Union* 82, 133–136.
- Burnett, B., Chanton, J., Christoff, H., Kontar, E., Krupa, S., Lambert, M., Moore, W., O'Rourke, D., Paulsen, R., Smith, C., Smith, L., & Taniguchi, M. (2002). Assessing methodologies for measuring groundwater discharge to the ocean. *EOS, Transactions, American Geophysical Union* 83, 117–123.
- Bussmann, I., Dando, P. R., Niven, S. J., & Suess, E. (1999). Groundwater seepage in the marine environment: role for mass flux and bacterial activity. *Marine Ecology Progress Series* 178, 169–177.
- D'Andrea, A. F., Aller, R. C., & Lopez, G. R. (2002). Organic matter flux and reactivity on a South Carolina sandflat: the impact of porewater advection and macrobiological structures. *Limnology and Oceanography* 47, 1056–1070.
- Demarest, J. M. (1978). *The shoaling of Breakwater Harbor, Cape Henlopen Area, Delaware Bay, 1842–1971*. Delaware Sea Grant College Program, Technical Report, DEL-SG-1-78, University of Delaware, Newark, DE.
- Emery, K. O. (1961). A simple method for measuring beach profiles. *Limnology and Oceanography* 6, 90–93.
- Fetter, C. W. (1994). *Applied hydrogeology* (3rd ed.). Englewood Cliffs: Prentice-Hall.
- Fitzgerald, D. M., Baldwin, C. T., Ibrahim, N. A., & Humphries, S. M. (1992). Sedimentologic and morphologic evolution of a beach-ridge barrier along an indented coast, Buzzards Bay, Massachusetts. In C. H. Fletcher, & J. F. Wehmiller (Eds.), *Quaternary coasts of the United States: Marine and Lacustrine systems, Special publication no. 48* (pp. 65–75). Tulsa: Society of Economic Paleontologists and Mineralogists.
- Freeze, R. A., & Cherry, J. A. (1979). *Groundwater*. Englewood Cliffs: Prentice-Hall.
- Garrels, R. M., & Mackenzie, F. T. (1971). *Evolution of sedimentary rocks*. New York: Norton.
- Glibert, P. M., & Loder, T. C. (1977). *Automated analysis of nutrients in seawater: A manual of techniques*. Technical Report WHOI-77-47, Woods Hole Oceanographic Institution, Woods Hole, MA.
- Grasshoff, K., & Johansen, J. (1972). A new sensitive and direct method for the automatic determination of ammonia in seawater. *Journal de Conseil, Conseil International pour l'Exploration de la Mer* 34, 516–521.
- Hansen, H. C. B., Wetsche, T. P., Raulund-Rasmussen, K., & Borggaard, O. K. (1994). Stability constants for silicate adsorbed to ferrihydrite. *Clay Minerals* 29, 341–350.
- Johannes, R. E., & Hearn, C. J. (1985). The effect of submarine groundwater discharge on nutrient and salinity regimes in a coastal lagoon off Perth, Western Australia. *Estuarine, Coastal and Shelf Science* 21, 789–800.
- Karrh, R. R., & Miller, D. C. (1996). Effect of flow and sediment transport on feeding rate of a surface-deposit feeder *Saccoglossus kowalevskii*. *Marine Ecology Progress Series* 130, 125–134.
- Kawabe, M., Sharp, J. H., Wong, K.-C., & Lebo, M. E. (1988). *Oceanographic data report number 8. Density profiles from the*

- Delaware Estuary, October 1986–September 1988. Delaware Sea Grant College Program Report DEL-SG-07-90, University of Delaware, Newark, DE.
- Klump, J. V., & Martens, C. S. (1983). Benthic nitrogen regeneration. In E. J. Carpenter, & D. G. Capone (Eds.), *Nitrogen in the marine environment* (pp. 411–457). New York: Academic Press.
- Kraft, J. C. (1971). *A guide to the geology of Delaware's coastal environments* (220 pp.). Newark: College of Marine Studies, University of Delaware.
- Krom, M. D., & Berner, R. A. (1980). Adsorption of phosphate in anoxic marine sediments. *Limnology and Oceanography* 25, 257–266.
- Landon, M. K., Rus, D. L., & Harvey, F. E. (2001). Comparison of instream methods for measuring hydraulic conductivity in sandy sediments. *Ground Water* 39, 870–885.
- Lanyon, J. A., Eliot, I. G., & Clarke, D. J. (1982). Groundwater-level variation during semidiurnal spring tidal cycles on a sandy beach. *Australian Journal of Marine and Freshwater Research* 33, 377–400.
- Leatherman, S. P. (1987). Coastal geomorphological applications of ground penetrating radar. *Journal of Coastal Research* 3, 397–399.
- Lee, D. R. (1977). A device for measuring seepage flux in lakes and estuaries. *Limnology and Oceanography* 22, 140–147.
- Li, L., Barry, D. A., Stagnitti, F., & Parlange, J.-Y. (1999). Submarine groundwater discharge and associated chemical input to a coastal sea. *Water Resources Research* 35, 3253–3259.
- Marshall, T. J., Holmes, J. W., & Rose, C. W. (1996). *Soil physics* (3rd ed.). Cambridge: Cambridge University Press.
- Maumeyer, E. M. (1974). *Analysis of short- and long-term elements of coastal change in a simple spit system: Cape Henlopen, Delaware*. MS thesis, University of Delaware, Newark, DE.
- Meyers, R. A., Smith, D. G., Jol, H. M., & Hay, M. B. (1994). Internal structure of a Pacific coast barrier spit using ground penetrating radar. *Fifth international conference on ground penetrating radar, proceedings, Vol. 2* (pp. 843–854).
- Miller, D. C., Bock, M. J., & Turner, E. J. (1992). Deposit and suspension feeding in oscillatory flow and sediment fluxes. *Journal of Marine Research* 50, 489–520.
- Miller, D. C., & Ullman, W. J. (2004). Ecological consequences of estuarine groundwater discharge at Cape Henlopen, Delaware Bay, USA. *Ground Water* (in review).
- Moore, W. S. (1996). Large groundwater inputs to coastal waters revealed by <sup>226</sup>Ra enrichments. *Nature* 380, 612–614.
- Moore, W. S. (1999). The subterranean estuary: a reaction zone of ground water and sea water. *Marine Chemistry* 65, 111–125.
- Officer, C. B. (1979). Discussion of the behaviour of non-conservative dissolved constituents in estuaries. *Estuarine and Coastal Marine Science* 9, 91–94.
- Officer, C. B., & Lynch, D. R. (1981). Dynamics of mixing in estuaries. *Estuarine, Coastal and Shelf Science* 12, 525–533.
- Page, H. M. (1995). Variation in natural abundance of <sup>15</sup>N in the halophyte, *Salicornia virginica*, associated with groundwater subsidies of nitrogen in a southern California salt-marsh. *Oecologia* 104, 181–185.
- Ray, A. J. (1989). *Influence of sediment dynamics and deposit feeding on benthic microalgae*. MS thesis, College of Marine Studies, University of Delaware, Lewes, DE.
- Redfield, A. C., Ketchum, B. H., & Richards, F. A. (1963). The influence of organisms on the composition of sea-water. In M. N. Hill, *The sea Vol. 2* (pp. 26–77). New York: Wiley.
- Sharp, J. H. (1988). Trends in nutrient concentrations in the Delaware Estuary. In S. K. Majumdar, E. W. Miller, & L. E. Sage (Eds.), *Ecology and restoration of the Delaware River Basin* (pp. 78–92). Philadelphia: The Pennsylvania Academy of Science.
- Sharp, J. H., Culbertson, C. A., & Church, T. M. (1982). The chemistry of the Delaware Estuary: general considerations. *Limnology and Oceanography* 27, 1015–1028.
- Sharp, J. H., Pennock, J. R., Church, T. M., Tramontano, J. M., & Cifuentes, L. A. (1984). The estuarine interaction of nutrients, organics, and metals: a case study in the Delaware Estuary. In V. S. Kennedy (Ed.), *The Estuary as a filter* (pp. 241–257). New York: Academic Press.
- Shaw, T. (2001). Conference provides forum for discussion of subterranean coastal environments. *EOS, Transactions, American Geophysical Union* 82, 622.
- Shepherd, R. G. (1989). Correlations of permeability and grain size. *Ground Water* 27, 633–638.
- Smith, S. V., & Atkinson, M. J. (1994). Mass balance of nutrient fluxes in coastal lagoons. In B. J. Kjerfve (Ed.), *Coastal lagoon processes* (pp. 133–155). New York: Elsevier.
- Strickland, J. D. H., & Parsons, T. R. (1972). *A practical handbook of seawater analysis* (2nd ed., 310 pp). Fisheries Research Board of Canada.
- Tobias, C. R., Macko, S. A., Anderson, I. C., Canuel, E. A., & Harvey, J. W. (2001). Tracking the fate of a high concentration groundwater nitrate plume through a fringing marsh: a combined groundwater tracer and in situ isotope enrichment study. *Limnology and Oceanography* 46, 1977–1989.
- Uchiyama, Y., Nadaoka, K., Rölke, P., Adachi, K., & Yagi, H. (2000). Submarine groundwater discharge into the sea and associated transport in a sandy beach. *Water Resources Research* 36, 1467–1479.
- Ullman, W. J., & Welch, S. A. (2002). Organic ligands and feldspar dissolution. In: R. Hellmann, & S. A. Wood (Eds.), *Water–rock interactions, ore deposits, and environmental geochemistry: A tribute to David Crerar. Special publication 7*. St. Louis: The Geochemical Society. pp. 3–35.
- Valiela, I. (1995). *Marine ecological processes* (2nd ed.). New York: Springer.
- Valiela, I., Foreman, K., LaMontagne, D., Hersh, D., Costa, J., Peckol, P., DeMeo-Anderson, B., D'Avanzo, C., Babione, M., Sham, C.-H., Brawley, J., & Lajtha, K. (1992). Couplings of watersheds and coastal waters: sources and consequences of nutrient enrichment of Waquoit Bay. *Estuaries* 15, 433–457.
- Vempati, R. K., & Loeppert, R. H. (1989). Influence of structural and adsorbed Si on the transformations of synthetic ferrihydrite. *Clays and Clay Minerals* 37, 273–279.
- Winter, T. C., Labaugh, J. W., & Rosenberry, D. O. (1988). The design and use of a hydraulic potentiometer for direct measurement of differences in hydraulic head between ground water and surface water. *Limnology and Oceanography* 33, 1209–1214.
- Zektzer, I. S., Ivanov, V. A., & Meskheteli, A. V. (1973). The problem of direct groundwater discharge to the seas. *Journal of Hydrology* 20, 1–36.